

Primary red bed magnetization revealed by fluvial intraclasts

Nicholas L. Swanson-Hysell¹, Luke M. Fairchild¹, Sarah P. Slotznick¹

¹ Department of Earth and Planetary Science, University of California, Berkeley, CA, USA

This article is to be submitted for consideration at GEOLOGY (published by the Geological Society of America).

¹ ABSTRACT

The magnetization of hematite-bearing sedimentary rocks provides critical records of geomagnetic reversals and paleogeography. However, the timing of hematite remanent magnetization acquisition is typically difficult to constrain and has led to much controversy in the interpretation of such data. This so-called “red bed controversy” stems from the reality that while detrital hematite in sediment can lead to a primary depositional remanent magnetization, alteration of minerals through interaction with oxygen can lead to the post-depositional formation of hematite. Growth of hematite crystals within sediments could occur in a geologically short time period immediately following deposition or could occur thousands to millions of years later due to the passage of oxygenated fluids following burial. Given that many paleomagnetic field tests such as the reversal test and fold test could still “pass” in scenarios with secondary post-depositional hematite growth, this problem has been particularly intractable in many sedimentary successions. In this study, we use an exceptionally well-preserved fluvial sediments within the 1.1 billion-year-old Freda Formation to gain insight into the timing of hematite remanence acquisition. This deposit contains siltstone intraclasts that were eroded from a coexisting lithofacies and redeposited within channel sandstone. Thermal demagnetization and petrographic data from these clasts reveal that they contain two generations of hematite. One population of hematite demagnetized at the highest unblocking temperatures and records directions that

19 rotated along with the rip-up clasts. This component is a primary detrital remanent
20 magnetization that formed prior to the reorientation of the clasts within the river. The other
21 component is removed at lower unblocking temperatures and has a consistent direction
22 throughout the intraclasts. This component is held by a population of finer-grained hematite that
23 grew and acquired a chemical remanent magnetization following deposition. The data support the
24 interpretation that the magnetization of hematite-bearing sedimentary rocks held by >400 nm
25 grains is more likely to record magnetization from the time of deposition and can be successfully
26 isolated from co-occurring authigenic hematite.

27 INTRODUCTION

28 The magnetizations of hematite-bearing sedimentary rocks known as “red beds” have provided
29 ample opportunities for Earth scientists to gain insight into the ancient geomagnetic field and the
30 paleogeographic positions of sedimentary basins. However, with these opportunities has come
31 much scientific debate, leading to what has been referred to as the “red bed controversy” (Butler,
32 1992; Beck et al., 2003; Van Der Voo and Torsvik, 2012). This controversy stems from the reality
33 that hematite within sedimentary rocks can have two sources: 1) detrital grains that are within
34 the sediment at the time of deposition; 2) grains that grow *in situ* after the sediments have been
35 deposited.

36 How does one constrain the relative age of hematite within sedimentary rocks? Many of the
37 traditional paleomagnetic field tests are unable to differentiate between primary versus diagenetic
38 remanence. For example, a structural fold test can constrain that a remanence direction was
39 obtained prior to folding, but millions of years have typically passed between the deposition of a
40 sediment, its burial in a sedimentary basin, and such tectonic tilting. Dual polarity directions
41 through a sedimentary succession are commonly interpreted as providing assurance that the
42 remanence records primary or near-primary magnetization; however, hematite growth could occur
43 significantly after deposition during a period when the geomagnetic field was reversing.

44 Petrographic investigations are valuable, but it can be difficult to ascertain how much the
45 petrographically observed hematite contributes to the magnetization and to unambiguously
46 interpret whether observed grains are detrital or not (e.g. Elmore and Van der Voo, 1982). A
47 common approach to classify hematite grains within red beds is into a fine-grained pigmentary
48 population, typically interpreted to have formed within the sediment, and a coarser-grained
49 population that has been referred to in the literature as “specularite” (Butler, 1992; Van Der Voo
50 and Torsvik, 2012). Tauxe et al. (1980) showed that sediments with abundant red pigmentary
51 hematite in the Miocene Siwalik Group had lower thermal unblocking temperatures than grey
52 samples dominated by a coarser-grained phase of specular hematite. Observations such as these
53 have led to the practice of defining the characteristic remanent magnetization from
54 hematite-bearing sediments as that held by the highest unblocking temperatures (Van Der Voo
55 and Torsvik, 2012). The primary versus secondary nature of micron-scale “specularite” grains
56 that likely carry this remanence has been one of the largest sources of contention in the “red bed
57 controversy” (Van Houten, 1968; Tauxe et al., 1980; Butler, 1992; Van Der Voo and Torsvik,
58 2012).

59 What is needed to address the timing of remanence acquisition is a process that reorients the
60 sediment before it has been lithified. Two such processes that can occur within a siliciclastic
61 depositional environment and be preserved in the rock record are: 1) syn-sedimentary slumping
62 wherein coherent sediment is reoriented through soft-sediment folding in the surface environment
63 and 2) intraclasts comprised of the lithology of interest that have been redeposited within the
64 depositional environment. Sediments that have undergone reorienting sedimentary processes can
65 provide significant insight into whether magnetization was acquired before or after reorientation.

66 Tauxe et al. (1980) studied 7 cobble-sized clasts within the Siwalik Group that were
67 interpreted to have formed by cut-bank collapse and discovered that their magnetic remanence
68 was acquired prior to clast reorientation. An investigation by Purucker et al. (1980) on red beds
69 of the Triassic Moenkopi Formation of Arizona used multiple such processes to gain insight into

70 hematite acquisition. In their study, an intraformational landslide deposit with isoclinal folds of
71 hematite-bearing claystone revealed non-uniform directions upon blanket demagnetization to
72 650°C that cluster better when corrected for their tilt leading to a primary interpretation. Scatter
73 was also observed in intraformational conglomerate clasts weathered out of an underlying unit
74 upon blanket thermal demagnetization to 630°C. However, the lack of principal component
75 analysis makes it difficult to evaluate the coherency of the directions. Complicating matters,
76 Larson and Walker (1982) analyzed shale rip-up clasts in the same Moenkopi Formation and used
77 the fact that similar remanence directions were removed between clasts during thermal
78 demagnetization up to 645°C as support for the hypothesis that red beds rarely reflect the
79 geomagnetic field at the time of deposition. Evaluating the robustness of this result is hindered by
80 the cessation of thermal demagnetization before the Néel temperature of hematite and the lack of
81 principal component analysis. These limitations are found in many studies from this era of
82 research, when the red bed controversy was particularly fervent, as the work predates the
83 widespread application of principal component analysis in conjunction with systematic
84 progressive thermal demagnetization (Kirschvink, 1980; Van Der Voo and Torsvik, 2012).

85 In this study, we investigate cm-scale siltstone intraclasts within the Freda Formation that
86 were eroded by fluvial processes and redeposited amongst cross-stratified sandstones (Fig. 1).
87 High-resolution thermal demagnetization data on these clasts constrain the timing of hematite
88 acquisition by revealing a primary component that formed prior to the erosion of the clasts within
89 the depositional environment and a secondary component that formed following their redeposition.

90 GEOLOGICAL SETTING

91 The ~4 km thick Freda Formation was deposited in the Midcontinent Rift as it was thermally
92 subsiding following the cessation of widespread magmatic activity (Cannon and Hinze, 1992). The
93 fluvial sediments of the Freda Formation are part of the Oronto Group and were deposited
94 following the deposition of the alluvial Copper Harbor Conglomerate and the lacustrine Nonesuch

95 Formation (Ojakangas et al., 2001). A maximum age constraint on the Freda Formation of
 96 $1085.57 \pm 0.25/1.3$ Ma (2σ analytical/analytical+tracer+decay constant uncertainty; Fairchild
 97 et al., 2017) is provided by an U-Pb date of a lava flow within the underlying Copper Harbor
 98 Conglomerate. Abundant fine-grained red siltstones within the formation have a well-behaved
 99 magnetic remanence dominated by hematite (Henry et al., 1977).

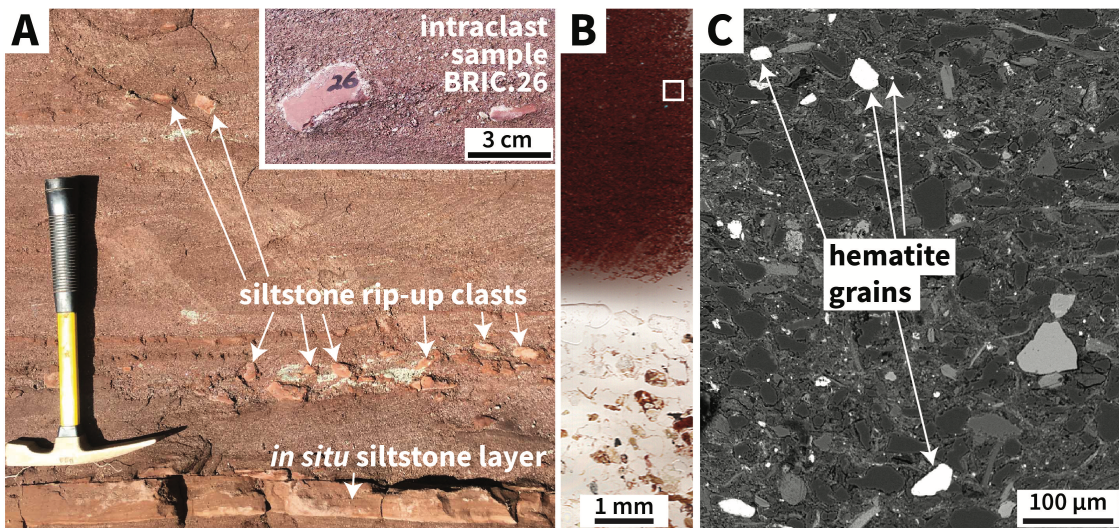


Figure 1. A: Siltstone intraclasts within the Freda Formation. The field photo shows an intact layer of siltstone below the hammer head which is topped by a bed of trough cross-stratified coarse sandstone with horizons of siltstone intraclasts. The hammer is 40 cm long. The inset photo is of an individual intraclast that was sampled as BRIC.26. B: A scan of a thin section of the BRIC.26 intraclast (upper half of image) and the coarse sand matrix (lower half of image). The red color of the intraclast is due to pigmentary hematite. C: Backscatter electron image of the siltstone clast from the region of the white box in B. The light-colored detrital grains (light due to iron's high atomic number) labeled with arrows were confirmed to be hematite through electron backscatter diffraction¹.

100 The studied outcrop is located along the Bad River (northern Wisconsin) in the lower portion
 101 of the Freda Formation – approximately 400 meters above its conformable base with the
 102 Nonesuch Formation.¹ The two main lithofacies in the studied outcrop are: (1) siltstone to very
 103 fine sandstone with planar lamination and horizons of ripple cross-stratification and (2) coarse to
 104 very coarse subarkosic sandstone with dune-scale trough cross-stratification (Fig. 1). These
 105 lithofacies are consistent with a fluvial depositional environment where the coarse sandstone facies

¹GSA Data Repository item 2018XXX, is available online at www.geosociety.org/pubs/ft2018.htm, or on request from editing@geosociety.org or Documents Secretary, GSA, P.O. Box 9140, Boulder, CO 80301, USA.

106 are channel deposits and the siltstones are inner-bank or over-bank deposits. The coarse-grained
107 sandstone contains horizons of tabular cm-scale intraclasts comprised of the dark red siltstone
108 lithology that is present in underlying beds of intact siltstone (Fig. 1). These tabular clayey-silt
109 intraclasts were eroded within the depositional environment and redeposited in the sandstone.
110 Due to migrating channels in fluvial systems, it is expected for a river to erode its own sediments.
111 The intraclasts would have been held together through cohesion resulting from the clay
112 component within the sediment. Given that the clasts are large (1 to 7 cm) relative to their host
113 sediment, and that they would have been fragile at the time of deposition, it is unlikely that they
114 were transported far.

115 METHODS and RESULTS

116 Oriented samples were collected and analyzed from 39 Freda Formation intraclasts. The
117 dimensions of the sampled clasts range from 2.2 x 1.4 x 0.5 cm to 7.2 x 2.3 x 1.2 cm. Given that
118 the clasts were typically smaller than the 1-inch-diameter drill cores used for sampling, they were
119 collected along with their sandstone matrix. These oriented cores were mounted onto quartz glass
120 discs with Omega CC cement and the matrix material was micro-drilled away. The mounted
121 clasts underwent stepwise thermal demagnetization in the UC Berkeley Paleomagnetism Lab
122 using an ASC demagnetizer (residual fields <10 nT) with measurements made on a 2G
123 DC-SQUID magnetometer. The demagnetization protocol had high resolution (5°C to 2°C to
124 1°C) approaching the Neél temperature of hematite resulting in 30 total thermal demagnetization
125 steps (Fig. 2). All paleomagnetic data are available to the measurement level in the MagIC
126 database (<https://earthref.org/MagIC/doi/>). *So that reviewers have access to the data, they are*
127 *currently available in CIT lab format and MagIC format here:*
128 https://github.com/Swanson-Hysell-Group/2018_Red_Bed_Intraclasts.

129 The clasts typically reveal two distinct magnetization directions. One direction was similar
130 throughout the intraclasts and was typically removed between 200°C and 650°C (Fig. 2). This

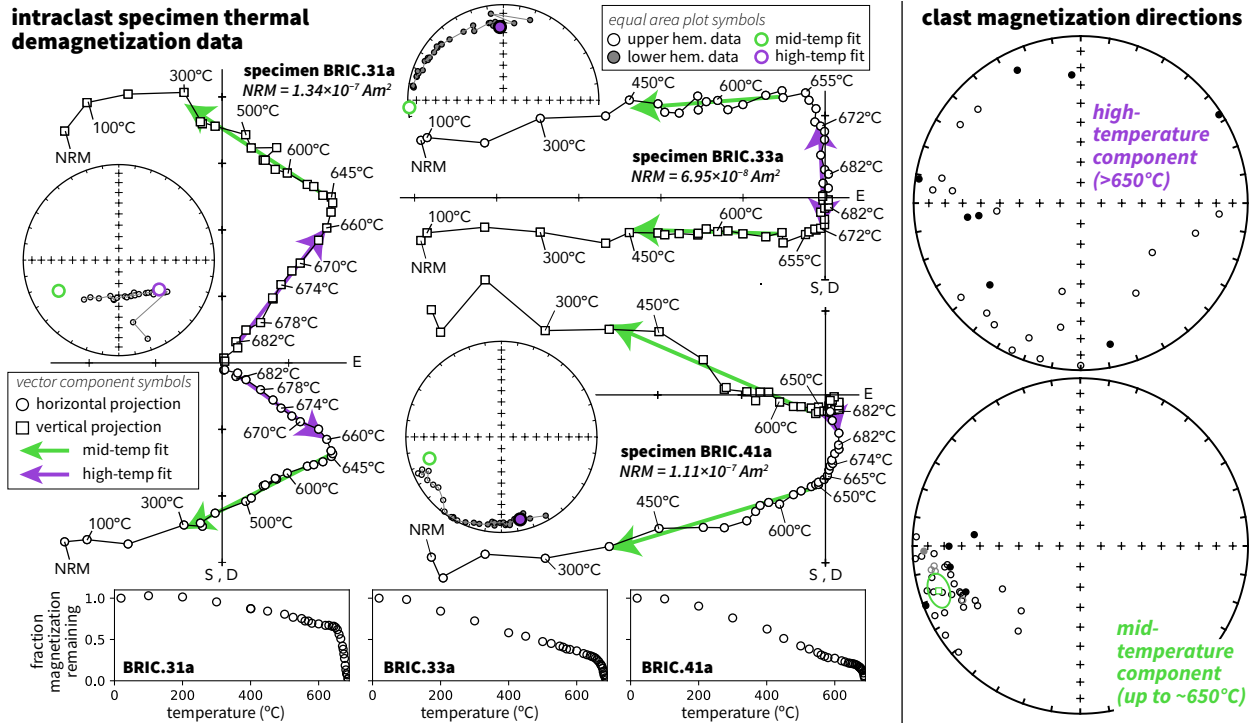


Figure 2. Paleomagnetic data from intraclasts reveal a mid-temperature component that typically unblocks prior to 655°C and a high-temperature component that typically unblocks between 655°C and 687°C. These components are present as varying fractions of the overall remanence as seen in the three individual clasts for which data are shown on vector component plots and measurement-level equal area plots in tilt-corrected coordinates (developed using PmagPy; Tauxe et al., 2016). The direction of the mid-temperature component is shown as purple arrows on the vector component plots and purple circles on the equal area plots while the high-temperature component is shown with green symbols. The mid-temperature component has a similar direction throughout the clasts as can be seen on the component directions equal area plots (mean declination: 252.4, inclination: -12.5, α_{95} : 6.6). In contrast, the high-temperature component directions are dispersed.

131 mid-temperature component is continuously unblocked between these temperatures with no or
 132 minimal downward inflection at $\sim 580^\circ\text{C}$ that would indicate remanence associated with magnetite
 133 (Fig. 2). This component is directionally well-grouped indicating that it was acquired following
 134 deposition of the clasts (Fig. 2). The other component trends towards the origin and is removed
 135 by thermal demagnetization steps at the highest levels such that it typically can be fit by a
 136 least-square line between 665°C and 688°C. The relative magnitude of the components varies
 137 between intraclasts (Fig. 2). While the high-temperature component can sometimes be fit as a
 138 line with a lower temperature bound of 660°C (BRIC.31a in Fig. 2), due to overlapping

139 unblocking temperatures between the mid-temperature and high-temperature components the
140 lower bounds of the high-temperature fits sometimes need to be as high as 680°C (BRIC.41a in
141 Fig. 2). Note that while the Neél temperature of hematite is sometimes given as 675°C in the
142 paleomagnetic literature, experimental data often show the Neél temperature to be as high as
143 690°C (Özdemir and Dunlop, 2006). There is typically a significant directional change in the
144 specimen magnetization between the mid-temperature component and the high-temperature
145 component (Fig. 2). As a result, 29 of the 39 analyzed intraclast specimens could be fit with
146 distinct mid-temperature and high-temperature least-squares lines. An additional 5 specimens
147 were undergoing directional change through the highest thermal demagnetization steps indicative
148 of the presence of a distinct high-temperature component, but this component was not
149 well-expressed enough to be fit. 5 of the specimens showed no directional change and could be fit
150 with a single mid-high-temperature component that is grouped with the mid-temperature
151 component. In contrast to the well-grouped mid-temperature component, the high-temperature
152 component directions are dispersed, indicating that the component was acquired prior to erosion
153 and redeposition of the clasts. The high-temperature component directions are more dispersed in
154 declination than inclination leading to a distribution that is not randomly dispersed on a sphere.
155 Given that the clasts are tabular and were liberated along their depositional lamination and
156 subsequently landed roughly bedding-parallel, it is to be expected that the rotations were largely
157 around a vertical axis which would preferentially change declination.

158 Petrography on the intraclasts reveals two distinct populations of hematite (Fig. 1). One
159 population is fine-grained pigmentary hematite present dominantly within the clay-sized matrix
160 and rimming detrital silt-sized grains. The zones of pigmentary hematite within the matrix
161 remain cloudy to high magnification indicating that the grains are submicron in size. The other
162 population of hematite has similar sizes and shapes to other detrital silt-sized grains – typically
163 ranging from 2 to 50 μm in diameter. These hematite grains were identified through reflected
164 light microscopy with their mineralogy supported by energy-dispersive x-ray spectroscopy (EDS)
165 and confirmed by electron backscatter diffraction (EBSD).

¹⁶⁶ **DISCUSSION**

¹⁶⁷ Single-domain hematite grains have high coercivities (>150 mT; Özdemir and Dunlop, 2014) and
¹⁶⁸ high unblocking temperatures. As a result, populations of hematite within rocks are stable on
¹⁶⁹ long timescales, resistant to overprinting, and therefore attractive for paleomagnetic study. In
¹⁷⁰ contrast to magnetite, hematite grains retain stable single-domain behavior in crystals $>1\mu\text{m}$
¹⁷¹ with the threshold to multidomain behavior occurring when grain diameters exceed $\sim 100\mu\text{m}$
¹⁷² (Kletetschka and Wasilewski, 2002; Özdemir and Dunlop, 2014). Hematite nanoparticles with
¹⁷³ diameters <30 nm have superparamagnetic behavior wherein thermal fluctuation energy
¹⁷⁴ overwhelms the ability of the grain to retain a stable magnetization at Earth surface temperatures
¹⁷⁵ (Özdemir and Dunlop, 2014). Hematite grains become progressively less influenced by thermal
¹⁷⁶ fluctuations as they reach grain sizes of a few hundred nanometers at which point they are stable
¹⁷⁷ up to temperatures approaching the Néel temperature of $\sim 685^\circ\text{C}$ (Swanson-Hysell et al., 2011;
¹⁷⁸ Özdemir and Dunlop, 2014). As a result, there is a strong relationship between grain volume and
¹⁷⁹ unblocking temperature that can be utilized to estimate grain size. A hematite population that is
¹⁸⁰ progressively unblocking at thermal demagnetization steps well below the Néel transition
¹⁸¹ temperature, such as the mid-temperature component of the intraclasts, is comprised of grains
¹⁸² within the ~ 30 to ~ 400 nm size range. This fine-grain size is consistent with the pigmentary
¹⁸³ phase within the intraclasts (Fig. 1).

¹⁸⁴ Given the directional consistency of the mid-temperature component among the intraclasts,
¹⁸⁵ this component must have dominantly formed as a chemical remanent magnetization after the
¹⁸⁶ intraclasts were redeposited in the channel. Chemical remanent magnetization acquisition by
¹⁸⁷ pigmentary hematite would have occurred as hematite grains grew to sizes above the
¹⁸⁸ superparamagnetic to stable single-domain transition resulting in the wide range of unblocking
¹⁸⁹ temperatures that is observed. In contrast, given its sharp unblocking temperature close to the
¹⁹⁰ Néel temperature, the high-temperature component is dominantly held by hematite grains that
¹⁹¹ are >400 nm such as the silt-sized hematite grains observed petrographically (Fig. 1). The

192 high-temperature remanence component held by these grains was rotated along with the clasts
193 indicating that it is primary and was acquired prior to the redeposition of the cohesive silt clasts.
194 That this component is held by larger grains sizes supports it being a detrital remanent
195 magnetization rather than a chemical remanent magnetization that formed very early prior to
196 clast erosion.

197 Oxidation of iron in aqueous environments often proceeds through the formation of
198 fine-grained poorly crystalline ferrihydrite, which transforms to stable crystalline hematite at
199 neutral pH on geologically short timescales (Cudennec and Lecerf, 2006). The broad unblocking
200 temperatures we observe for the chemical remanent magnetization in the Freda intraclasts are
201 similar to those in hematite populations produced through experimental ferrihydrite to hematite
202 conversion (Jiang et al., 2015). The differential unblocking temperature spectra of the two
203 components within the Freda intraclasts provides strong support for the argument of Jiang et al.
204 (2015) that chemical and detrital remanent magnetization can be distinguished; due to detrital
205 remanence unblocking at the highest temperatures. However, it is also clear from the Freda
206 intraclast data that while the detrital remanent magnetization can be well-isolated at
207 temperatures as low as 650°C (specimen BRIC.31a in Fig. 2), the chemical remanent
208 magnetization thermal unblocking spectra can overlap with that of the detrital remanence and
209 extend up to temperatures closer to the Néel temperature (specimen BRIC.41a in Fig. 2).
210 Therefore, to isolate primary remanence in red beds, best practice should be to proceed with very
211 high resolution thermal demagnetization steps above 600°C, and particularly above 650°C. These
212 intraclast data reveal that directional change at the highest unblocking temperatures provides an
213 effective means to discriminate primary and secondary magnetizations within siltstones of the
214 Freda formation and other red beds. The formation of coarse-grained secondary hematite can
215 occur, particularly in high permeability lithologies and deeply weathered profiles. However, the
216 isolation of primary detrital hematite in >1 billion-year-old siltstones lends confidence to
217 magnetostratigraphic records and paleogeographic interpretations that are based on
218 interpretations of primary magnetization in ancient red beds.

219 **ACKNOWLEDGEMENTS**

220 This research was supported by the Esper S. Larsen, Jr. Research Fund and the National Science Foundation
221 through grant EAR-1419894. SPS was supported by the Miller Institute for Basic Research in Science. The
222 Wisconsin Department of Natural Resources granted a research and collection permit that enabled sampling within
223 Copper Falls State Park. Oliver Abbitt assisted with field work, Taiyi Wang assisted with paleomagnetic analyses
224 and Tim Teague provided technical support for EBSD analyses.

225 **References**

- 226 Beck, M. E., Burmester, R. F., and Housen, B. A., 2003, The red bed controversy revisited: shape analysis of
227 Colorado Plateau units suggests long magnetization times: *Tectonophysics*, vol. 362, pp. 335–344,
228 doi:10.1016/s0040-1951(02)00644-3.
- 229 Butler, R., 1992, *Paleomagnetism: Magnetic Domains to Geologic Terranes*: Blackwell Scientific Publications.
- 230 Cannon, W. F. and Hinze, W. J., 1992, Speculations on the origin of the North American Midcontinent rift:
231 *Tectonophysics*, vol. 213, pp. 49–55, doi:10.1016/0040-1951(92)90251-Z.
- 232 Cudennec, Y. and Lecerf, A., 2006, The transformation of ferrihydrite into goethite or hematite, revisited: *Journal*
233 *of Solid State Chemistry*, vol. 179, pp. 716–722, doi:10.1016/j.jssc.2005.11.030.
- 234 Elmore, R. D. and Van der Voo, R., 1982, Origin of hematite and its associated remanence in the Copper Harbor
235 Conglomerate (Keweenawan), upper Michigan: *J. Geophys. Res.*, vol. 87, pp. 10,918–10,928,
236 doi:10.1029/JB087iB13p10918.
- 237 Fairchild, L. M., Swanson-Hysell, N. L., Ramezani, J., Sprain, C. J., and Bowring, S. A., 2017, The end of
238 Midcontinent Rift magmatism and the paleogeography of Laurentia: *Lithosphere*, vol. 9, pp. 117–133,
239 doi:10.1130/L580.1.
- 240 Henry, S., Mauk, F., and der Voo, R. V., 1977, Paleomagnetism of the upper Keweenawan sediments: Nonesuch
241 Shale and Freda Sandstone: *Canadian Journal of Earth Science*, vol. 14, pp. 1128–1138, doi:10.1139/e77-103.
- 242 Jiang, Z., Liu, Q., Dekkers, M. J., Tauxe, L., Qin, H., Barrón, V., and Torrent, J., 2015, Acquisition of chemical
243 remanent magnetization during experimental ferrihydrite–hematite conversion in earth-like magnetic
244 field—implications for paleomagnetic studies of red beds: *Earth and Planetary Science Letters*, vol. 428, pp.
245 1–10, doi:10.1016/j.epsl.2015.07.024.
- 246 Kirschvink, J., 1980, The least-squares line and plane and the analysis of paleomagnetic data: *Geophysical Journal*
247 of the Royal Astronomical Society, vol. 62, pp. 699–718, doi:10.1111/j.1365-246x.1980.tb02601.x.
- 248 Kletetschka, G. and Wasilewski, P. J., 2002, Grain size limit for SD hematite: *Physics of the Earth and Planetary*
249 *Interiors*, vol. 129, pp. 173–179, doi:10.1016/S0031-9201(01)00271-0.
- 250 Larson, E. E. and Walker, T. R., 1982, A rock magnetic study of the lower massive sandstone, Moenkopi Formation
251 (Triassic), Gray Mountain Area, Arizona: *Journal of Geophysical Research: Solid Earth*, vol. 87, pp. 4819–4836,
252 doi:10.1029/jb087ib06p04819.
- 253 Ojakangas, R. W., Morey, G. B., and Green, J. C., 2001, The Mesoproterozoic Midcontinent Rift System, Lake
254 Superior Region, USA: *Sedimentary Geology*, vol. 141–142, pp. 421–442, doi:10.1016/s0037-0738(01)00085-9.
- 255 Özdemir, Ö. and Dunlop, D. J., 2006, Magnetic memory and coupling between spin-canted and defect magnetism in
256 hematite: *J. Geophys. Res.*, vol. 111, doi:10.1029/2006JB004555.
- 257 Özdemir, Ö. and Dunlop, D. J., 2014, Hysteresis and coercivity of hematite: *Journal of Geophysical Research: Solid*
258 *Earth*, vol. 119, pp. 2582–2594, doi:10.1002/2013JB010739.
- 259 Purucker, M. E., Elston, D. P., and Shoemaker, E. M., 1980, Early acquisition of characteristic magnetization in red
260 beds of the Moenkopi Formation (Triassic), Gray Mountain, Arizona: *Journal of Geophysical Research*, vol. 85,
261 p. 997, doi:10.1029/jb085ib02p00997.
- 262 Swanson-Hysell, N. L., Feinberg, J. M., Berquó, T. S., and Maloof, A. C., 2011, Self-reversed magnetization held by
263 martite in basalt flows from the 1.1-billion-year-old Keweenawan rift, Canada: *Earth and Planetary Science*
264 *Letters*, vol. 305, pp. 171–184, doi:10.1016/j.epsl.2011.02.053.

- 265 Tauxe, L., Kent, D. V., and Opdyke, N. D., 1980, Magnetic components contributing to the NRM of Middle Siwalik
266 red beds: *Earth and Planetary Science Letters*, vol. 47, pp. 279–284, 10.1016/0012-821X(80)90044-8.
- 267 Tauxe, L., Shaar, R., Jonestrask, L., Swanson-Hysell, N., Minnett, R., Koppers, A., Constable, C., Jarboe, N.,
268 Gaastra, K., and Fairchild, L., 2016, PmagPy: Software package for paleomagnetic data analysis and a bridge to
269 the Magnetics Information Consortium (MagIC) Database: *Geochemistry, Geophysics, Geosystems*,
270 doi:10.1002/2016GC006307.
- 271 Van Der Voo, R. and Torsvik, T. H., 2012, The history of remagnetization of sedimentary rocks: deceptions,
272 developments and discoveries: Geological Society, London, Special Publications, vol. 371, pp. 23–53,
273 doi:10.1144/SP371.2.
- 274 Van Houten, F. B., 1968, Iron oxides in red beds: *Geological Society of America Bulletin*, vol. 79, p. 399,
275 doi:10.1130/0016-7606(1968)79[399:ioirb]2.0.co;2.